

1 Long Term Performance of the Pierre Auger 2 Observatory

Koun Choi^{*a} for the Pierre Auger Collaboration^b

^aUniversité Libre de Bruxelles, Brussels, Belgium

^bObservatorio Pierre Auger, Av. San Martín Norte 304, 5613 Malargüe, Argentina

E-mail: auger_spokespersons@fnal.gov

Full author list: http://www.auger.org/archive/authors_icrc_2019.html

The Pierre Auger Observatory is the largest detector ever built to measure ultra high energy cosmic rays. It employs a hybrid technique combining a surface detector consisting of 1660 water-Cherenkov stations and a fluorescence detector composed of 27 Schmidt telescopes. The construction of the Observatory started in 2004 and since then it has been continuously taking data in a stable manner. We will present the behavior of the Observatory over more than 14 years and the expected response into the future with the AugerPrime upgrade now underway. Key performance indicators such as the on-time and the event rates will be presented. The instruments for calibration and monitoring of the detectors will also be reviewed.

*36th International Cosmic Ray Conference — ICRC2019
24 July – 1 August, 2019
Madison, Wisconsin, USA*

*Speaker.

1. Overview of the Pierre Auger Observatory

The Pierre Auger Observatory (PAO) is the world's largest cosmic ray air-shower detector. The Observatory is built on 3000 km² high plain in the province of Mendoza, Argentina. It adopts a hybrid design which combines a Surface Detector (SD) consisting of 1660 water-Cherenkov stations and a Fluorescence Detector (FD) composed of 27 Schmidt telescopes deployed at four different sites overlooking the SD array. The SD captures the lateral spread of the Extensive Air Showers (EAS) at ground level, while the FD observes their longitudinal profiles.

The construction of the SD started in January 2004, and it has been running in full configuration since 2008. After the completion of the SD-1500 with 1.5 km spacing between the stations placed in a triangular grid, the lower energy extension of the SD, *SD-750 array*, has started. It comprises of 61 stations with a grid spacing of 750 m. It started taking data in 2011. An SD station is composed of a water tank of 3.6 m diameter and 1.2 m height housing a liner bag made from reflective Tyvek. The liner bag is filled with ultra-pure water, and three 9-inch photomultiplier tubes (PMTs) optically coupled to the purified water are looking downwards into the tank. When relativistic charged particles from an air-shower pass through the inner volume, emitted Cherenkov light is reflected on the inner Tyvek surface and detected by the PMTs. Each station is equipped for autonomous operation with a solar power battery and pannel, a front-end electronics board, GPS, and communication antennae. The Cherenkov light observed by each PMT is digitized at 40 MHz by 10 bit Flash Analog-to-Digital Convertor (FADC) channels for the output from the last PMT dynode and the anode.

The FD detects nitrogen fluorescence light induced by the electromagnetic component of the EAS in the atmosphere. A single telescope has a field of view of ($30^\circ \times 30^\circ$) in azimuth and elevation angles, with the minimum elevation of 1.5° above horizon. The combination of the six telescopes in each site covers 180° in azimuth angle. By a spherical mirror of 3.4 m radius of curvature, light is focused on a camera composed of 440 hexagonal PMTs assembled in a (22×20) matrix taking data at a frequency of 10 MHz. The number of photons detected by each camera pixel is converted to the number of emitted photons considering the energy deposited in the atmosphere. Twelve fluorescence telescopes in the Los Leones and Coihueco sites started data taking in January 2004. Another six telescopes launched in May 2005 in the Los Morados site, and at last, six telescopes in the Loma Amarilla site became operational in March 2007. Since September 2009, three additional telescopes (HEAT: High Elevation Auger Telescope) with an elevated field of view ($30^\circ \div 60^\circ$) have been also operating to study lower energy cosmic rays.

The atmosphere is the medium where the EAS develop and thus an important part of the Observatory is dedicated to measuring the atmospheric conditions and the amount of dust and aerosols present in the air. LIDARs (Laser Imaging Detection and Ranging) are used to measure the vertical aerosol optical depth and the atmospheric horizontal uniformity, Infrared cameras are providing the cloud coverage, balloons are launched for measuring the atmospheric profile. Details on the design and previous studies on the performance of the Observatory can be found in [1].

Currently the Observatory is undergoing the AugerPrime upgrade program whose major aim is to enhance the sensitivity of the SD to the mass composition at the highest energies by deployment of the SSD (Surface Scintillator Detector) on top of the SD water tank. The upgrade plan also includes a radio detector deployment, the AMIGA (Auger Muons and Infill for the Ground Array)

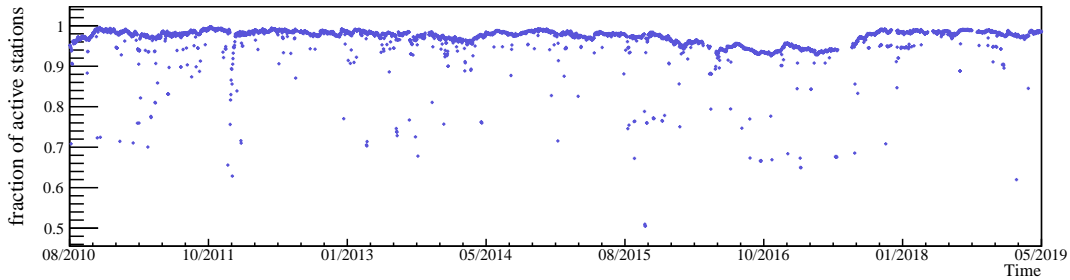


Figure 1: Number of functioning SD stations normalized to the number of deployed SD stations as a function of time.

45 project, as well as an increase of the duty cycle of the FD [2]. Thus it is important to ensure that
 46 the detector will continue to take high quality data in the next decade.

47 The functioning of the SD, the FD and the other instruments is constantly monitored, from
 48 observables related to the PMTs to higher level variables used in advanced analysis. In this work
 49 we will provide an information of long term performance of the PAO by reviewing its behavior
 50 over more than 14 years. In section 2, we will describe the performance of the SD and the expected
 51 performance in the next decade of operation. We will review the performances of the FD and of
 52 the calibration and atmosphere monitoring instruments in section 3 and conclude in section 4.

53 2. Long term performance of the Surface Detector

54 The surface detector is exposed to unstable weather conditions such as large temperature vari-
 55 ation, lightning, high salinity, dusts and humidity. These environmental conditions can damage the
 56 detector and influence the quality of data. To constantly monitor the detector condition and re-
 57 sponse, various sensors are installed in every SD station. Variables related to temperature, battery
 58 power, PMT voltage and current, dynode/anode ratio (the ratio of the amplitude of the output from
 59 the last PMT dynode to the one from the anode) are sent to the Central Data Acquisition System
 60 (CDAS) and then exported to a MySQL database (DB) server [1, 3, 4].

61 Besides monitoring the conditions of the station hardware, the number of triggers a station is
 62 transmitting is continuously watched. Each station has two levels of triggers (called $T1$ and $T2$).
 63 Due to the limited data transmission bandwidth the trigger algorithms are implemented locally in
 64 the station's software. The $T2$ trigger selects signals with amplitudes exceeding a threshold (TH),
 65 or signals that are spread in time (*time over threshold* or ToT). The $T2$ triggers are sent to CDAS
 66 to form the trigger for air-showers based on time and spacial coincidence between the signals.
 67 Details of the triggers can be found in [5]. Irrespective of any air-shower trigger the status of
 68 the array is monitored on a minute basis. The number of active stations which are able to send
 69 $T2$ signals are constantly monitored. The ratio between the active stations to the total number of
 70 deployed stations is depicted in Fig. 1. Since the beginning of the deployment, on average more
 71 than 95% of all stations have been functioning. Lower values correspond to DAQ down time,
 72 communication issues in the data transmission to CDAS or other on-site problems occasionally

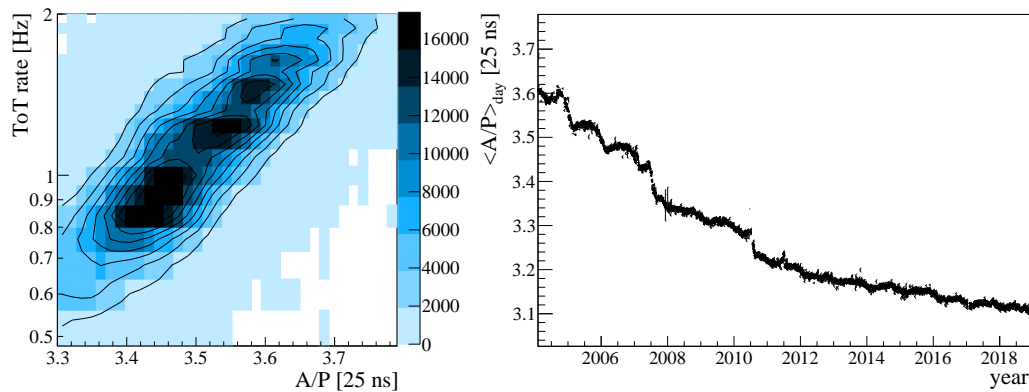


Figure 2: *Left:* Correlation between AoP and ToT using monitoring data from October 2006. *Right:* Daily average of the area over peak of one of the 3 PMTs (pmt id 3) in the station Rocio (station id 270) as a function of time.

73 occurring for individual stations. The interval of time when the entire array was not transmitting
 74 data amounts to less than 1% since 2004.

75 The particles produced by the air-showers initiated by cosmic rays of low energies pass through
 76 the stations at a rate of about 3000 per second, providing a constant flux for the calibration and for
 77 the monitoring of the stations. Selected by a simple threshold trigger, the amplitude and the charge
 78 of each signal are piled up in individual histograms for each PMT. The calibration histograms are
 79 filled during one minute. Among the particles entering the tank, the muons, because of their longer
 80 path in the detectors produce a larger amount of Cherenkov photons and provide a distinctive larger
 81 area and a higher peak than the electrons and photons. These values are computed in the station
 82 software and then sent to CDAS each six minutes. The entire calibration histograms are transmitted
 83 to CDAS with each triggered air-shower. By employing the spacial uniform flux of the atmospheric
 84 muons a uniform calibration for the entire array is achieved.

85 The change in the light distribution and amplitude of the recorded signals has a direct influence
 86 on the trigger rate. A good variable to assess and understand the slow changes in the detectors is the
 87 area over peak (A/P) of the atmospheric muon signals. This variable is related to the reflectivity of
 88 the Tyvek liner and transparency of the water as well as the response of PMTs and of the electron-
 89 ics. The correlation between the ToT trigger which depends on the shape of the muon pulse and
 90 therefore on the A/P is illustrated in Fig.2 (left). The right plot of the Fig. 2 is an example of the
 91 A/P evolution showing a typical behavior, of 1 PMT in station Rocio which has been taking data
 92 since 2004. After deployment, most stations experience a rapid decrease of the A/P, followed by a
 93 milder slope which tends for become flat. An annual modulation related to the seasonal tempera-
 94 ture and pressure variation is also seen. In 2007 and 2010, part of the stations experienced sudden
 95 drops, which are correlated to very cold winters with temperature drops below -10° Celsius [6].
 96 In the last 9 years the freezing temperatures in winters did not influence anymore the A/P behavior.
 97 For example in the winter of 2018 the temperatures dropped below -10° Celsius and no significant
 98 drops have been observed.

99 The stacked distribution of the A/P loss is shown in the left plot of Fig. 3. For each A/P profile

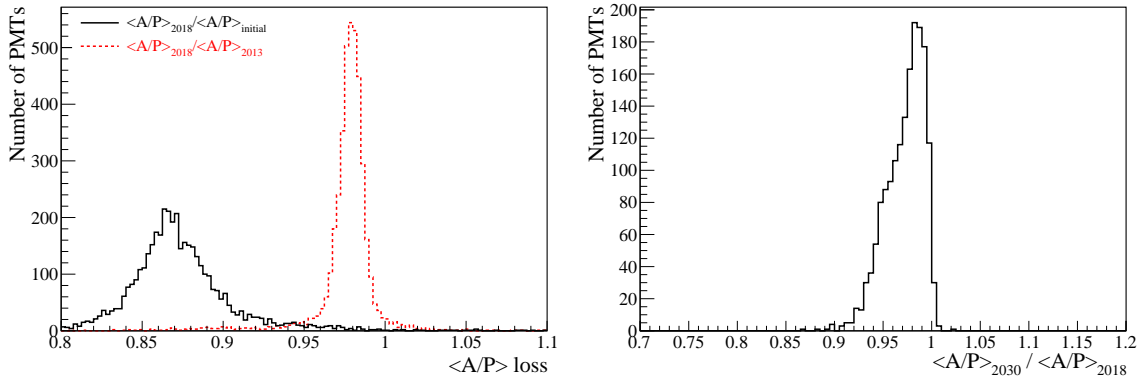


Figure 3: *Left:* Stacked distribution of A/P loss, defined as $\langle A/P \rangle_{2018}$ of each PMT divided by $\langle A/P \rangle_{initial/2013}$ of each PMT. *Right:* $\langle A/P \rangle$ expected in 2030 divided by the current $\langle A/P \rangle$.

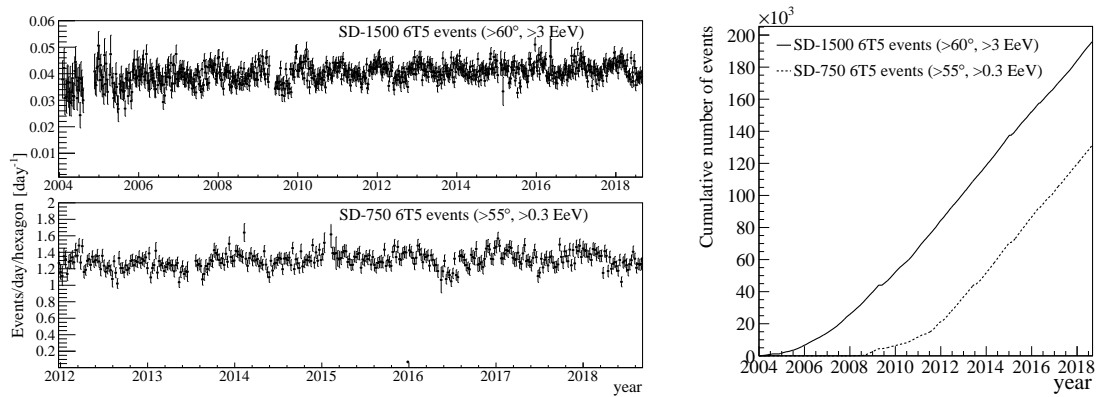


Figure 4: *Left:* Evolution of the daily 6T5 rate normalized to the number of hexagons. *Top:* number of the SD-1500 array events without above $>3 \times 10^{18}$ eV and zenith angle $<60^\circ$. *Bottom:* number of the SD-750 array events above $>3 \times 10^{18}$ eV and zenith angle $<55^\circ$. *Right:* Cumulative number of 6T5 events

100 the average A/P in 2018 is computed and the A/P loss is defined as a ratio of the value with respect
 101 to the initial deployment year. Among the 4175 PMTs used in the evaluation, less than 18.5% of
 102 the PMTs have experienced a decrease of more than 15% compared to their initial values. Shown
 103 in the same plot is the stacked distribution of the A/P loss since 2013. In the last 5 years the A/P
 104 have stabilized, with a loss of less than 5% for 95% of the PMTs.

105 The long-term evolution of the A/P is described by a model characterizing the exponential
 106 decay combined with an annual modulation [6]. The A/P evolution is extrapolated to estimate the
 107 expected A/P in future. By selecting PMTs with data points of more than 5 months and without
 108 a discontinuity in the recent two years of data, 1655 PMTs are fitted with the model. In 2030,
 109 85% of these PMTs are expected to have A/P larger than 95% of their current values. Based on
 110 this extrapolation we can assume that in the operation time of Auger the surface detectors will not
 111 experience a significant change in their behavior.

112 As the decrease of the A/P influences the station trigger it is important to asses if there are

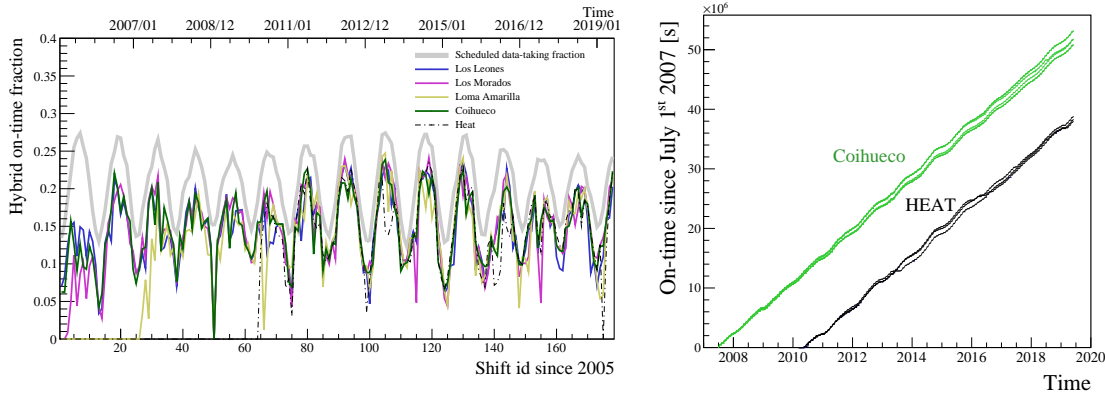


Figure 5: *Left:* The on-time fraction is shown for the four FD sites (Los Leones, Los Morados, Loma Amarilla and Coihueco) and the HEAT for hybrid events. The X-axis is drawn for shift ID, where in principle each shift covers a moon cycle. *Right:* The accumulated on-time since July 1, 2007 for 6 telescopes of Coihueco and 3 telescopes of HEAT.

113 any effects on air-shower trigger. The air-shower trigger is formed by requiring a time coincidence
 114 between at least three neighbouring stations ($T3$ trigger). More details on the triggering system
 115 can be found in [5]. A quality trigger, called $6T5$ trigger, ensuring the selection of events well
 116 contained in the array and thus with accurate reconstruction, requires that at the time of the event
 117 all six neighbouring stations of the station with the highest signal in an event are active. The $6T5$
 118 events are the basis of high-level analysis like the measurements of the energy spectrum [7]. For
 119 cosmic rays with zenith angle less than 60° and energy larger than 3 EeV , the trigger efficiency
 120 for the SD-1500 array is 100%. For the SD-750 array, full efficiency is achieved above 0.3 EeV
 121 and less than 55° . The time evolution of the daily rate of $6T5$ events per hexagon and passing the
 122 full trigger efficiency conditions is shown in Fig. 4 (left), the error bars representing the statistical
 123 uncertainties. As can be seen, even if the stations have experienced an A/P decrease the rate is
 124 constant over more than 14 years, being 0.040 ± 0.004 events/day/hexagon for the SD-1500 array
 125 and 1.3 ± 0.1 events/day/hexagon for the SD-750 array. In 2013 new station triggers have been
 126 implemented in the software which do not depend strongly on the shape of the signal. Being sen-
 127 sitive to small signals they lower the energy threshold for full efficiency of the arrays and assuring
 128 a constant event rate above this threshold.

129 The cumulative number of $6T5$ events is illustrated in Fig. 4(right). The SD has been running
 130 with high efficiency of data accumulation through the 15 years of the data taking history. The SD-
 131 1500 data sets contain currently more than 4.5 million $6T5$ events out of which more than 450.000
 132 are above 3 EeV .

133 3. Long term performance of the Fluorescence Detector

134 The fluorescence telescopes operate during moonless, clear nights. For their data taking, it
 135 is required that the sun is lower than 18° below the horizon (evening and morning astronomical
 136 twilights) and the moon is below the horizon for longer than three hours, and the moon fraction is
 137 lower than 70% in the middle of the night. The sky photon background flux (Night Sky Brightness)

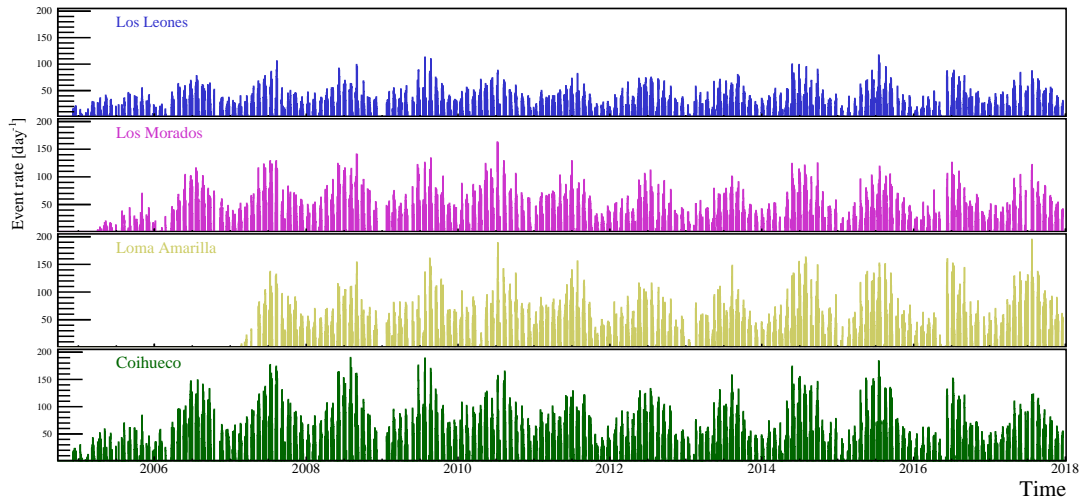


Figure 6: Number of events taken in each day are shown for the four FD sites, respectively.

138 and the artificial lights in the field of view of the FD telescopes should also be marginal. The data
 139 taking is also sensitive to weather conditions such as rain, snow, strong winds and lightnings.

140 A monitoring database stores information from the Slow Control System which continuously
 141 monitors detector and weather conditions.

142 When an EAS is observed by the FD in coincidence with at least one SD station, it allows
 143 better shower geometry reconstruction than its detection by the FD alone. These events are called
 144 *hybrid events* and knowing the hybrid on-time is crucial for an accurate evaluation of the exposure.
 145 The time evolution of the on-time fraction of the hybrid events is shown in Fig. 5 (left) for four
 146 FD sites and the HEAT telescopes. The on-time of the hybrid detector is compared to the nominal
 147 Data Acquisition (DAQ) time which is the desired data taking time fraction calculated based on the
 148 Sun and the Moon positions as previously described. In addition to the Night Sky Brightness and
 149 the weather conditions, technical problems such as DAQ failure can cause inefficiency of the FD
 150 operation. After the initial phase of each telescope, the mean of the on-time has been maintained to
 151 be about 13% for all FD sites. Seasonal modulation is also visible since nights are longer in winter.
 152 Calculation of the on-time fraction is described in detail in [8]. On the right side of Fig. 5, the
 153 accumulated on-time in second since July 1, 2007 for Coihueco and HEAT telescopes is shown.

154 The daily number of hybrid events observed by individual FD sites are shown in Fig. 6 as a
 155 function of time. The continuous data has been successfully achieved, also seasonal modulation is
 156 visible as for the on-time distribution.

157 To monitor the long-term performance of each optical devices, three light sources are injected
 158 to three different destinations on each telescope and operated before and after the operation of tele-
 159 scopes. By comparing measurements from the three light sources, abnormality of camera pixels,
 160 mirror and aperture components can be identified.

161 The reconstruction of the air-shower longitudinal profiles requires conversion of an ADC count
 162 in each camera pixel to light flux. Such absolute energy calibration of the FD is achieved by
 163 delivering calibration campaigns with a drum-shaped tool, in which pulsed UV LED illuminating
 164 the interior of the 2.5 m diameter cylindrical drum of 1.4 m depth.

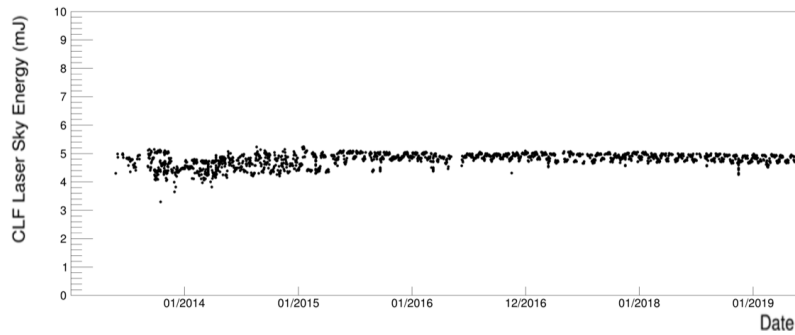


Figure 7: The CLF laser sky energy [mJ] as a function of time. (needed a pdf version and/or a root macro)

165 Understanding atmospheric condition near the ground as well as horizontal atmospheric pro-
 166 files is important for the reconstruction of the air-shower profiles. Especially atmospheric trans-
 167 mission through aerosols needs a rigorous monitoring due to their large and fast time variation and
 168 the significant effect on the air-shower reconstruction [1]. The Central Laser Facility (CLF) and the
 169 eXtreme Laser Facility (XLF) continuously take data to monitor the aerosol optical depth vertical
 170 profiles in the FD field of view on an hourly basis [9]. During the FD data acquisition, the two
 171 facilities vertically shot a set of 50 collimated UV laser pulses every 15 minutes, which can be
 172 simultaneously detected by multiple FD telescopes. The CLF has been in operation since 2003 and
 173 a major upgrade was done in 2013 to add a beam calibration system and a backscatter Raman lidar
 174 receiver. For the absolute calibration of the CLF beam, the entire beam is captured with an external
 175 radiometer before and after each night's operation. Figure 7 illustrates the sky energy of the CLF
 176 beam measured by the calibration system. For more information about the CLF and XLF facilities
 177 and the analyses, refer to [1, 9].

178 4. Conclusion

179 We presented the long-performance of the Pierre Auger Observatory over more than 15 years
 180 of data taking history. Key performance indicators such as the on-time and event rates of the accu-
 181 mulated data are reviewed to be stable and efficient for both Surface and Fluorescence detectors.
 182 The instruments for calibration and monitoring of the detectors are also reviewed to operate stably.
 183 The study carried out on atmospheric muons shows that the area over peak reduction will be less
 184 than 5% for the most of the PMTs in the next decade. The overall event rate above the current
 185 threshold ($\sim 3 \times 10^{18}$ EeV for the SD-1500 array) for full efficiency will therefore remain constant
 186 for the future data taking.

187 References

- 188 [1] The Pierre Auger Collaboration, Nucl. Instr. Meth. A 798 (2015)
 189 [2] The Pierre Auger Collaboration, arXiv:1604.03637 [astro-ph.IM]
 190 [3] X. Bertou *et al.* for the Pierre Auger Collaboration, Nucl. Instrum. Meth. A **568**, 839 (2006)
 191 [4] C. Bonifazi for the Pierre Auger collaboration, ICRC (2013) 1079

- 192 [5] The Pierre Auger Collaboration, Nucl. Instrum. Meth. A **613**, 29 (2010)
193 [6] R. Sato for the Pierre Auger collaboration, ICRC (2011) 204
194 [7] V. Verzi for the Pierre Auger collaboration, PoS(ICRC2019) 450
195 [8] P. Abreu, et al., Astropart. Phys. 34 (2011)
196 [9] V. Harvey for the Pierre Auger collaboration, PoS(ICRC2019) 283